

# **DEVELOPMENT OF THREE-DIMENSIONAL THERMO-MECHANICAL FINITE ELEMENT MODEL FOR PREDICTION OF THERMAL DEFORMATION DURING SELECTIVE LASER SINTERING PROCESS**

Mohammad Razzaghian, Ahmed Sherif El-Gizawy, Yuwen Zhang  
Mechanical and Aerospace Engineering, University of Missouri  
E3408 Lafferre Hall  
Columbia MO 65211

## **ABSTRACT**

The main advantages of 3D printing (additive layer manufacturing) over conventional methods are that it reduces costs by eliminating the need for tooling, enables faster production of prototypes and goods, and reduces waste because the excess powder can be reused. A common method for 3D printing using metal powder is selective laser sintering (SLS). In this technique, a model is created using a CAD software. A laser irradiates the powder and partially melts it layer by layer until the shape of the object is formed. Then, the liquid powder solidifies into the final object. During the phase changes, a temperature difference gradient between layers causes residual thermal stress. This thermal stress leads to shrinkage and warpage in the final products.

In this paper, a transient 3D thermo-mechanical model using finite element analysis (FEA) is applied in order to study thermal deformation in the partial melting process. The thermal deformation analysis is presented at different running times. The results for the thermal deformation analysis show that as the time increases, the degree of thermal deformation increases. The developed model sets the basis for a more comprehensive model for process-induced defects in laser-based 3D printing of metal powder.

## **1. INTRODUCTION**

### **1.1 Topic and scope**

The purpose of this paper is to explain the thermal deformation in the selective laser sintering process in detail. This is done by using Ansys Workbench 15.0. While efforts have been made to ensure the boundary conditions of the simulation match reality as closely as possible, real-world experimental results are outside the scope of this paper as it is impossible to observe the thermal deformation process millisecond by millisecond in real time.

### **1.2 Audience**

A graduate-level background in mechanical engineering is necessary to understand the contents of this paper. In addition, knowledge about thermodynamics and heat transfer are helpful to understand the mechanisms at work in the thermal deformation process. Readers should also be familiar with ALM in general and the SLS process in particular in order to benefit from this report, but a detailed knowledge of the processes is not required. The contents of this paper could be helpful to anyone who uses SLS in research, industry, etc.

### 1.3 Background regarding the SLS process

Additive layer manufacturing gets its name because unlike traditional manufacturing techniques that build parts by cutting material away, ALM creates them layer by layer [1]. There are many different methods by which the ALM process can occur. The differences mainly lie in the materials used and how the melting process occurs [2]. The method that will be discussed in this paper is selective laser sintering (SLS). This method was invented in the 1980's and is now widely used in a variety of industries such as dental science and aerospace engineering [3]. This process involves depositing powder layer by layer to create the finished product and using a powerful laser to melt the powder [1]. An advantage of SLS is that many different materials can be used: polymers (such as nylon), metals (such as titanium) [4].

### 1.4 Literature review

In ALM, an important cause of decreased quality in the final product is thermal deformation, which is caused by residual thermal stress. Though SLS is widely used in a variety of industries, the exact effects of thermal distortion on the final products has not been fully investigated [5]. In particular, the effects of complete melting on thermal distortion in ALM have been studied by researchers Paul, Anand, and Gerner [2], but the thermal FEA model assumed that the metal powder is completely melted to achieve perfectly dense parts. However, depending on the laser and material parameters, the powders may not be sintered perfectly, so the effects of partial melting on thermal distortion are still not clearly known.

Wang [6] developed a model for predicting the effect of shrinkage in the SLS process. Wang et al. [7] refined the model by studying the effect of process parameters on shrinkage. Senthilkumaran et al. [8] then created a new model which took into account part geometry and beam offset, which resulted in more accurate part production. Ning et al. [9, 10] were able to correlate hatch length and scan speed to shrinkage using an inverse regression equation, which allowed them to decrease part shrinkage. The in-plane and out-plane shrinkage was shown experimentally by Zhu et al. [11]. Kruth et al. [12] explained the shrinkage process in SLS by using the temperature.

Chen et al. [13] investigated the shrinkage effect in two powder. Since part quality is of utmost importance to manufacturing products, distortion and warpage received much attention from researchers in recent years. Measurement of thermal deformation in SLS has been studied experimentally by Pohl et al. [14]. A 3D finite element analysis with the fixed temperature boundary condition as a heat source was done by Ma et al. [15] in order to calculate the thermal stress and temperature gradient.

## 2. EXPERIMENTATION

### 2.1 Boundary conditions

The model was created using the CAD program SolidWorks. The model was then exported from SolidWorks into Ansys Workbench 15.0. Two different boundary conditions were set to perform a thermal (temperature distribution) analysis. The value for the heat flux for the inlet boundary condition is  $1e7 \text{ W/m}^2$ . The second boundary condition is that the bottom half of the sphere has zero heat flux. This is because the laser beam hits the top of the sphere; the energy is greatly reduced at the bottom of the sphere.

The temperature distribution provided by the thermal analysis serves as a boundary condition for the structural model. This boundary condition is called the imported body temperature. The thermal deformation is the result of applying this thermal load to the model.

Figure 1 and 2 show the faces that the boundary conditions have been applied to.

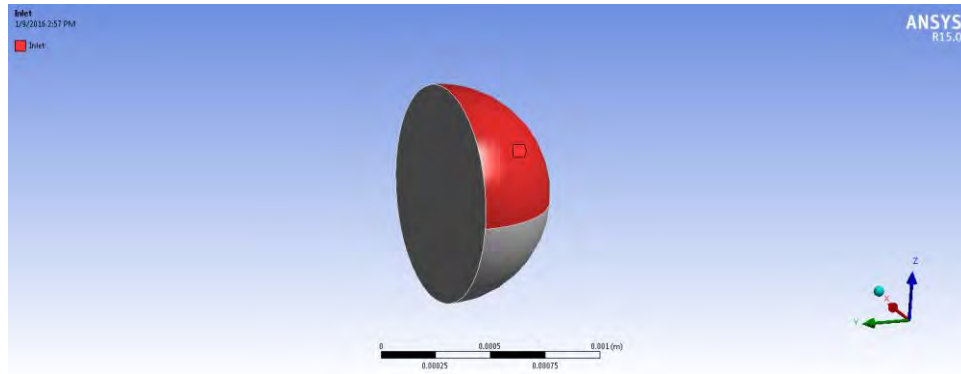


Figure 1. Inlet face

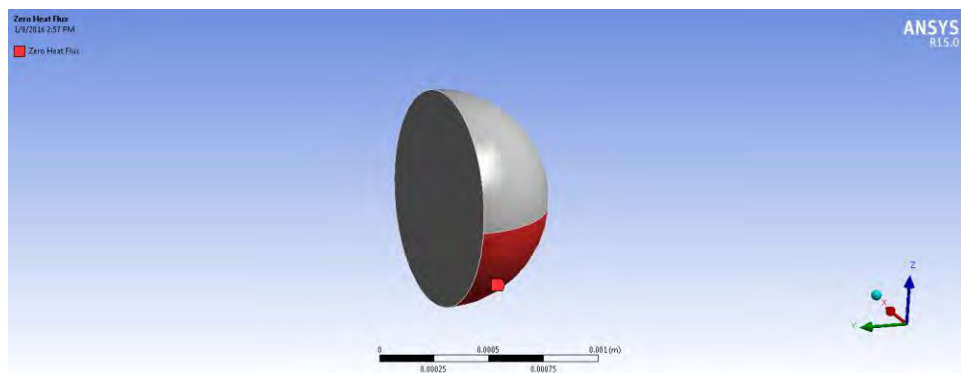


Figure 2. Zero heat flux

## 2.2 Thermomechanical finite element model

There are two thermomechanical analysis coupling methods used in simulation software. The first one is direct coupling, whereby the thermal and mechanical boundary conditions are set simultaneously, thus the result of thermomechanical analysis can be gotten in one step. The disadvantage of this method is that it is not supported by Ansys Workbench interface, which is well-suited to solving the problem of thermal deformation in SLS. An alternative method is called sequential coupling. This is the method that was used in this paper. This involves setting the boundary conditions for the thermal model and then using the result as a boundary condition for the structural model.

## 2.3 Material properties

The material used in this paper is titanium powder. The physical properties of titanium are listed in table 1. Titanium was chosen for this study because it is suitable to various industries, ranging from aerospace engineering to medical science due to its high strength-to-weight ratio and resistance to corrosion [16]. It is also one of the most biocompatible metals, which makes it a possibility for medical implants created by SLS [17].

Table 1. Physical properties of titanium

Properties of Titanium Powder Used in Ansys Workbench 15.0	
Density (kg/m <sup>3</sup> )	4430
Cp (Specific Heat (j/kg-k))	526
Thermal Conductivity (W/m-k)	6.7
Coefficient of Thermal Expansion (1/°C)	8.4E-6
Poisson's Ratio	0.32
Young's Modulus (Pa)	110.3E+9

## 3. RESULTS

### 3.1 Simulation process

In this study, the thermal deformation analysis is done using Ansys Workbench 15.0. This analysis is done in nine different times which are 2, 3, 4, 5, 6, 7, 8, 9, and 10 milliseconds. The time step size is 0.0001 seconds and the number of time steps is 10.

As is shown in Figure 3, the partial melting process started at 2 milliseconds. The maximum thermal deformation at this time is very low at 4.7066e-6 meters.

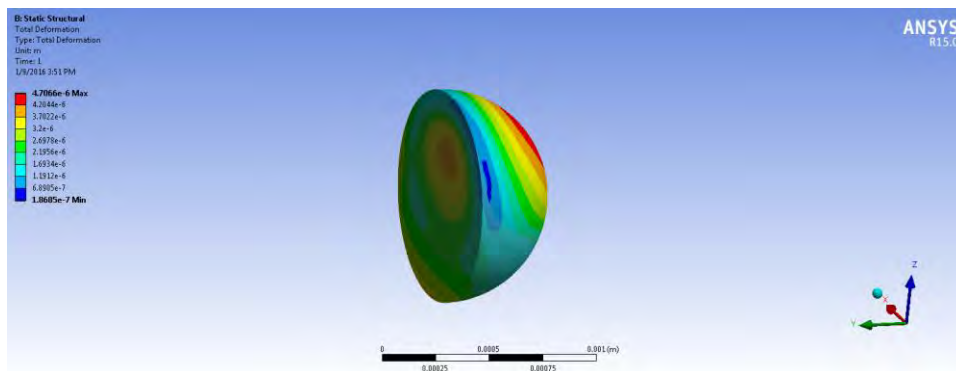


Figure 3. Thermal deformation analysis at 2 milliseconds

As can be seen from Figure 4, that the maximum thermal deformation at time equals to 3 milliseconds is 5.2806e-6 meters and also according to Figure 5 is 7.3067e-6 meters at time equals to 4 milliseconds. It can be understood that the thermal deformation in the part layers will

increase as time increases. It can be seen that the areas of maximum thermal deformation are concentrated near the top of the sphere, which is what one would expect in the SLS process since that is where the laser beam hits the model. It can also be seen that the thermal deformation increases rapidly between three and four milliseconds, especially in the top center of the sphere.

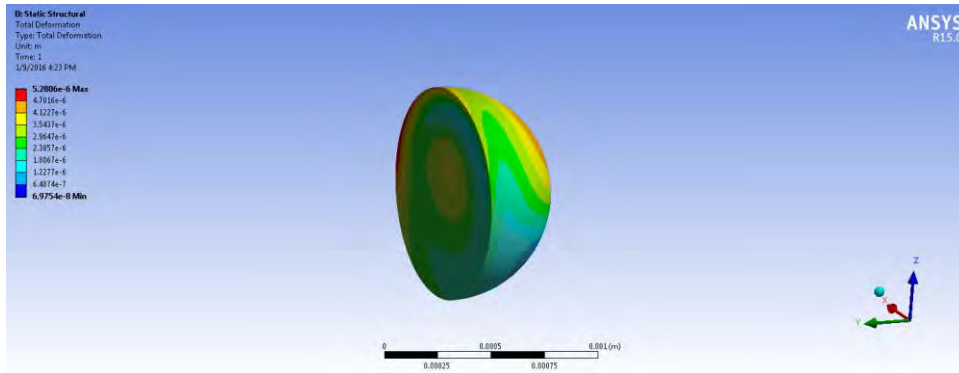


Figure 4. Thermal deformation analysis at 3 milliseconds

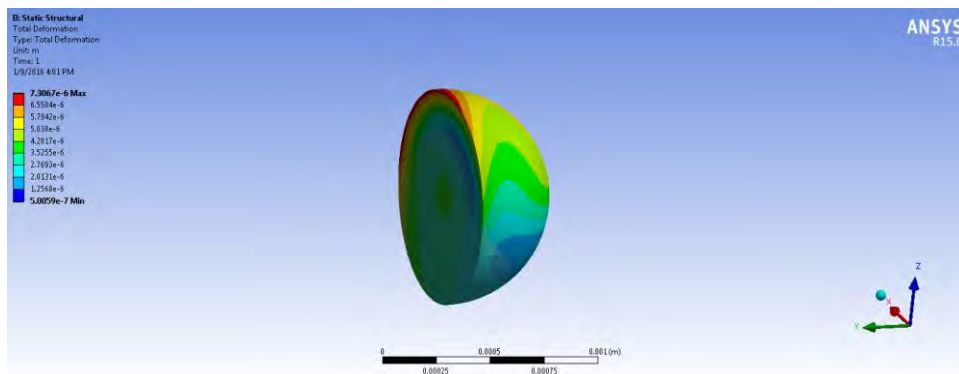


Figure 5. Thermal deformation analysis at 4 milliseconds

Figure 6 and 7 show the thermal deformation in the part layers at times equal to 5 and 6 milliseconds. It can be seen that at time equals to 5 milliseconds the maximum thermal deformation is  $9.9199 \times 10^{-6}$  meters whereas at 6 milliseconds it is  $1.2456 \times 10^{-5}$  meters. Also note that the minimum thermal deformation increases from  $2.5179 \times 10^{-7}$  meters to  $5.8082 \times 10^{-7}$  meters. That means the entire model is deforming, not just the areas that are under the highest heat flux.

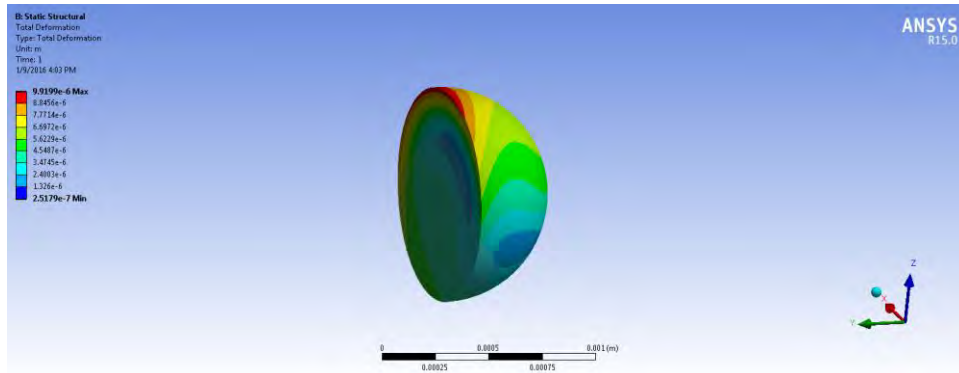


Figure 6. Thermal deformation analysis at 5 milliseconds

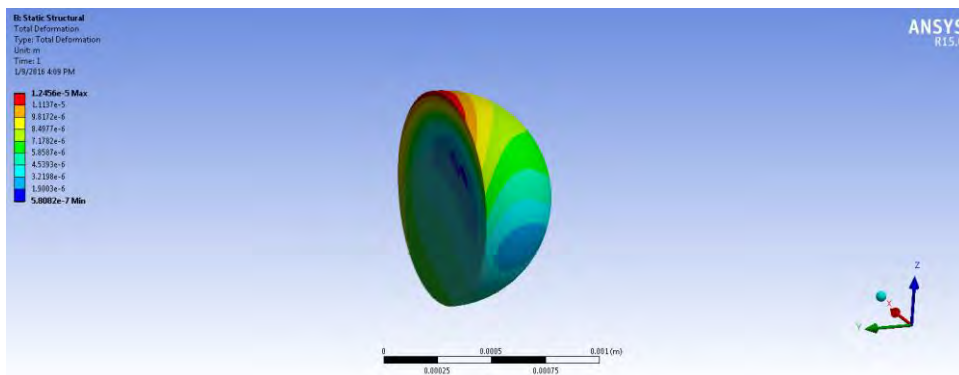


Figure 7. Thermal deformation analysis at 6 milliseconds

As is shown by the below figures, the maximum thermal deformation at 7 milliseconds is equal to  $1.4901 \times 10^{-5}$  meters and at 8 milliseconds is equal to  $1.7318 \times 10^{-5}$  meters.

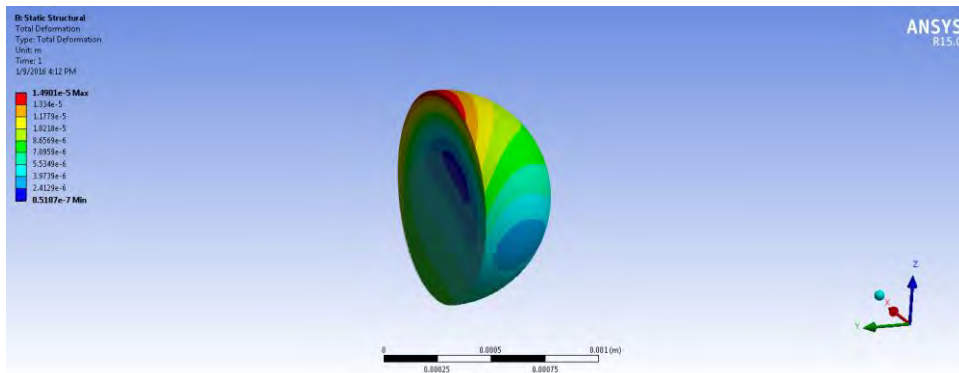


Figure 8. Thermal deformation analysis at 7 milliseconds

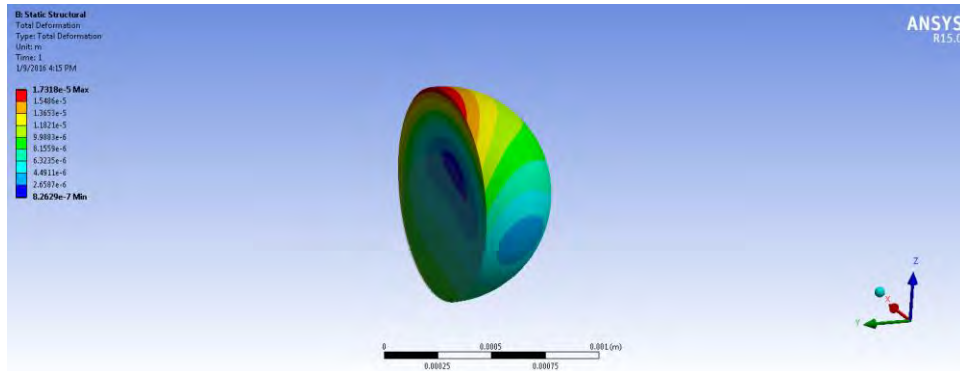


Figure 9. Thermal deformation analysis at 8 milliseconds

As shown in the below figures, the thermal deformation at 9 milliseconds is  $1.9662 \times 10^{-5}$  meters and at 10 milliseconds is  $2.2085 \times 10^{-5}$  meters. In Figures

10 and 11, it can be seen that the shaded areas are virtually identical, whereas between any previous 1 millisecond intervals, the colors changed. This is because the respective levels of deformation in certain parts of the sphere are stabilizing.

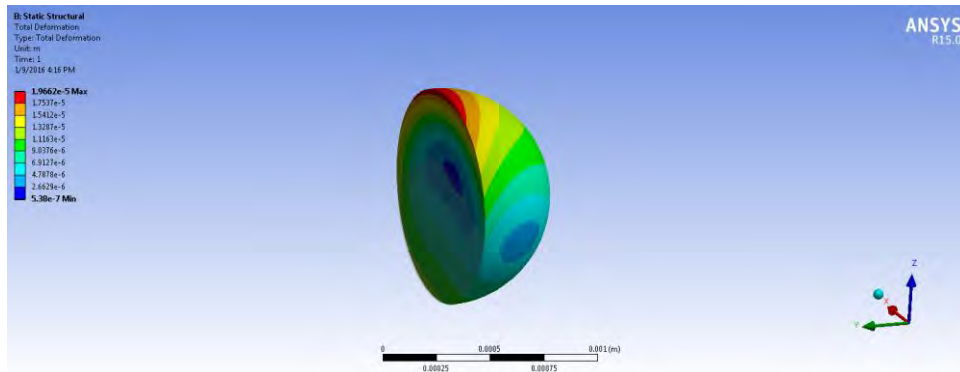


Figure 10. Thermal deformation analysis at 9 milliseconds

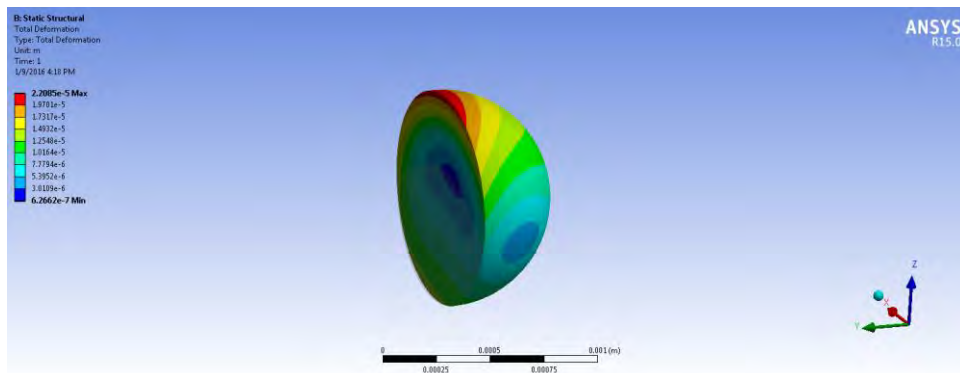


Figure 11. Thermal deformation at 10 milliseconds

## 4. CONCLUSIONS

### 4.1 Summary

In this study, a 3D transient model has been used by coupling a thermomechanical finite element model. This study has been done in the simulation software Ansys Workbench 15.0. The simulation has been run in different time steps with 1 millisecond intervals between them. The study shows that as the time increases, so does maximum thermal deformation. In order to validate these results, the model should be tested experimentally using a SLS 3D printer. The knowledge gained by studying the thermal deformation in SLS can be used to minimize the warpage and shrinkage of parts, and thus reduce the cost of producing parts.

## 5. REFERENCES

1. Introduction to 3D Printing, European Social Fund, Malta 2007-2013. Ministry for Education and Employment. <<https://education.gov.mt/en/resources/News/Documents/Youth Guarantee/3D Printing.pdf>>.
2. Paul R., Anand S. & Gerner, F. “Effect of thermal deformation on part errors in metal powder based additive manufacturing processes,” *Journal of Manufacturing Science and Engineering* 136 (2014):1-12.
3. Behrendt, U. & Shellabear, M. “The EOS rapid prototyping concept”. *Computers in Industry*, 1995: 57-61.
4. Despa V. & Gheorghe I. “Study of selective laser sintering – a qualitative and objective approach”, 2011.
5. Roberts, I. A. “Investigation of Residual Stress in the laser melting of metal powders in additive layer manufacturing”, 2012.
6. Wang, X. “Calibration of Shrinkage and Beam Offset in SLS Process,” *Rapid Prototyping Journal* 5(3) (1999): 129-133.
7. Wang, R., Wang, L., Zhao, L. & Liu Z. “Influence of Process Parameters on Part Shrinkage in SLS,” *International Journal of Advanced Manufacturing Technology* 33(5) (2007): 498-504.
8. Senthilkumaran, K., Pandey, P. M. & Rao, P. V. M. “New Model for Shrinkage Compensation in Selective Laser Sintering,” *Virtual and Physical Prototyping*, 4(2) (2009): 49-62.
9. Ning, Y., Wong, Y. S., Fuh, J. Y. H. & Loh, H. T. “An Approach to Minimize Build Errors in Direct Metal Laser Sintering,” *IEEE Transaction On Automation Science and Engineering* 3(1) (2006): 73-80.
10. Ning, Y., Wong, Y. S. & Fuh, J. Y. H. “Effect and Control of Hatch Length on Material Properties in the Direct Metal Laser Sintering Process,” *Journal of Engineering Manufacturing* 219(1) (2005): 15-25.
11. Zhu, H. H., Lu, L. & Fuh, J. Y. H. “Study on Shrinkage Behaviour of Direct Laser Sintering Metallic Powder,” *Journal of Engineering Manufacturing* 220(2) (2006): 183-190.

12. Kruth, J. P., Froyen, L., Van Vaerenbergh, J., Mercelis, P., Rombouts, M. & Lauwers, B. “Selective Laser Melting of Iron-Based Powder,” *Journal of Materials Processing Technology* 149(1-3) (2004): 616-622.
13. Chen, T. & Zhang, Y. “Three-Dimensional Modeling of Laser Sintering of a Two-Component Metal Powder Layer on Top of Sintered Layers,” *ASME Journal of Manufacturing Science and Engineering* 129(3) (2006): 575-582.
14. Pohl, H., Simchi, A., Issa, M. & Dias, H. C. “Thermal Stresses in Direct Metal Laser Sintering,” *Proceedings of the 12th Solid Freeform Fabrication Symposium*. University of Texas at Austin, August 6-8, 2001.
15. Ma L. & Bin H. “Temperature and stress analysis and simulation in fractal scanning-based laser sintering,” *International Journal of Advanced Manufacturing Technology* 34(9) (2007): 898-903.
16. Hosseini, A. & A. Kishawy, H. *Cutting Tool Material and Tool Wear*, 2014.
17. Elias C.N., J.H.C. Lima, R. Valiev. & M.A. Meyers. Biomedical Applications of Titanium and its Alloys, *Biological Materials Science*, 2008.